

Neprilysin controls the synaptic activity of neuropeptides in the intercalated cells of the amygdala

Authors:

Gregoriou GC, Patel SD, Winters BL, Bagley EE

Primary laboratory of origin:

Discipline of Pharmacology & Charles Perkins Centre, Charles Perkins Centre D17,
University of Sydney, Camperdown, NSW, 2006, Australia.

Running title: Neuropeptides degradation in the amygdala

Corresponding author: Elena Bagley

Address: Discipline of Pharmacology & Charles Perkins Centre, Charles Perkins Centre D17, University of Sydney, Camperdown, NSW, 2006, Australia.

Telephone: 61 2 93514895

Fax: N/A

E-mail: elena.bagley@sydney.edu.au

Number of pages: 31

Number of figures: 3

Number of references: 56

Words in abstract: 245

Words in introduction: 486

Words in discussion: 844

Abbreviations:

ACE: angiotensin-converting enzyme

ACSF: artificial cerebrospinal fluid

APN: aminopeptidase N

BLA: basolateral amygdala

CNS: central nervous system

DOR: δ -opioid receptor

EPSC: excitatory post-synaptic currents

MOR: μ -opioid receptor

met-enk: methionine enkephalin

NEP: neprilysin

N/OFQ: Nociceptin/Orphanin FQ

PI: peptidase inhibitors

PPR: paired pulse ratio

Abstract (250 word max)

Endogenous opioid peptides in the amygdala regulate many of our behaviours and emotional responses. In particular, the endogenous opioid enkephalin plays a significant role in regulating amygdala activity, but its action is strongly limited by peptidases which degrade enkephalin into inactive fragments. Inhibiting peptidases maybe an attractive method to enhance endogenous opioid signalling, however we do not know which specific peptidase/s to target. Using inhibition of glutamate release onto the intercalated cells of the amygdala as an assay for enkephalin activity, we applied specific peptidase inhibitors to determine which peptidase/s regulate enkephalin signalling in this region. Thiorphan (10 μ M), captopril (1 μ M) or bestatin (10 μ M) were used to inhibit the activity of neprilysin, angiotensin-converting enzyme or aminopeptidase N respectively. In rat brain slices containing the intercalated cells, we found that inhibition of glutamate release by a submaximal concentration of enkephalin was doubled by application of all three peptidase inhibitors combined. Then, we tested inhibitors individually and found that inhibition of neprilysin alone could enhance enkephalin responses to the same extent as inhibitors of all three peptidases combined. This indicates neprilysin is the predominant peptidase responsible for degrading enkephalins in the intercalated cells of the amygdala. This differs from the striatum, locus coeruleus and spinal cord, where multiple peptidases metabolise enkephalin. These data highlight the importance of knowing which specific peptidase/s control opioid actions in the relevant neural circuit and how they change in disease states, to allow rationale choices of drugs targeting the specific peptidase of interest.

Significance Statement (1-2 sentences, 80 word max)

Endogenous opioids modulate many of our emotional and behavioural responses. In the amygdala they modulate our pain, fear and addictive behaviours. Their actions are terminated when they are catabolised into inactive fragments by at least 3 different peptidases. In this study we found that neprilysin selectively controls endogenous opioid concentrations at synapses in the intercalated cells of the amygdala. This peptidase may be a target for regulation of endogenous opioid modulation of amygdala mediated emotional and behavioural responses.

Introduction

Endogenous opioid peptides in the central nervous system (CNS) modulate a number of complex physiological and pathophysiological states, including: pain perception, fear responses, attachment formation, drug addiction and decision-making (Lutz and Kieffer, 2013; Bodnar, 2018). Despite this broad influence, the conditions and precise mechanisms in which endogenous opioids regulate synaptic transmission are not well understood. The ability of endogenous opioids to regulate synaptic transmission is determined by a combination of three factors: the level of peptide release, opioid receptor activation and peptide degradation. The rapid degradation of endogenously released opioids by peptidases contributes to their short-lived biological activity. For example, the enkephalins, an endogenous opioid family with high affinity for μ - and δ -opioid receptors (MORs and DORs respectively), are rapidly cleaved into inactive peptide fragments in the brain and spinal cord by three main zinc-dependent metallopeptidases (Sullivan et al., 1978; Chou et al., 1984; Hiranuma and Oka, 1986; Hiranuma et al., 1997, 1998; Guyon et al., 1979). Neprilysin (NEP, EC 3.4.24.11) and angiotensin-converting enzyme (ACE, EC 3.4.15.1) cleave enkephalins at a high affinity site between the glycine-phenylalanine bond (Hiranuma and Oka, 1986; Hiranuma et al., 1997, 1998; Guyon et al., 1979; Erdos et al., 1978). In contrast, aminopeptidase N (APN, EC 3.4.11.2) cleaves enkephalins at a low affinity site between the tyrosine-glycine bond (Hersh, 1985, Figure 1A). Although these biochemical assays have assessed the vulnerability of enkephalin to each peptidase, the ability of each individual peptidase to curtail the cellular actions of enkephalin is not fully defined. In the locus coeruleus APN and, to a lesser extent, NEP, regulate enkephalin activation of G-protein gated inwardly rectifying potassium channels (Williams et al., 1987). Whereas in the spinal cord, the activity of multiple peptidases is required to regulate enkephalin induced internalisation of MOR into spinal cord neurons (Song and Marvizon., 2003). This suggests that even though all three peptidases are expressed widely throughout the central nervous system (Barnes et al.,

1988), there may be topographical specificity to peptidase control over endogenous opioid actions.

The amygdala is a brain region that is central to our emotional responses. In particular, the amygdala participates in our learned fear responses, our responses to pain and aspects of drug addiction (Janak and Tye, 2015) and endogenous opioids regulate all of these responses (Lutz and Kieffer, 2013; Bodnar, 2018). We have recently shown that the endogenous opioid enkephalin inhibits the synaptic inputs and excitability of the intercalated cells of the amygdala (Winters et al., 2017). A cocktail of peptidase inhibitors that targeted ACE, APN and NEP potentiated the actions of endogenous and exogenous enkephalin at glutamatergic synapses in the intercalated cells (Winters et al., 2017). In this exploratory study we tested the hypothesis that individual peptidases are responsible for enkephalin degradation at this synapse. To test this hypothesis, we used inhibition of glutamatergic synaptic inputs to the intercalated cells as an assay for enkephalin levels in order to determine how enkephalin levels are changed by application of specific peptidase inhibitors.

Materials and methods

Animals

All experiments were performed on male Sprague-Dawley rats (3–9 weeks) obtained from the Animal Resources Centre (Government of Western Australia, Perth, Australia). Rats were housed in groups of 6 in a low background noise room and maintained on a normal light/dark cycle (12 h/12 h) with *ad libitum* access to food and water. All experimental procedures were approved by the Animal Care Ethics Committee of the University of Sydney (protocols 2017/1257 & 2014/617) and were conducted in accordance with the Australian code of practice for the care and use of animals for scientific purposes.

Slice preparation

Rats were anaesthetised with isoflurane using the open drop method and then decapitated. The brain was swiftly removed and placed in ice-cold cutting solution of composition (in mM) 125 NaCl, 2.5 KCl, 1.25 NaH₂PO₄·2H₂O, 2.5 MgCl₂, 0.5 CaCl₂, 11 D-glucose and 25 NaHCO₃, and saturated with carbogen (95% O₂/5% CO₂). Coronal brain slices (280 μm) containing the rostral amygdala were cut with a vibratome (Leica Biosystems, Nussloch, Germany) and then maintained at 34 °C in a chamber containing carbogenated cutting solution. Slices were incubated in this chamber for an hour before being used for electrophysiological recordings. For recording, slices were transferred to a recording chamber that was continuously superfused with artificial cerebrospinal fluid (ACSF) containing (in mM): 125 NaCl, 2.5 KCl, 1.25 NaH₂PO₄·2H₂O, 1 MgCl₂, 2 CaCl₂, 11 D-glucose and 25 NaHCO₃, saturated with carbogen and heated to 32–34 °C. Neurons of interest were visualised using an upright Olympus BX51 microscope using Dodt gradient contrast optics.

Electrophysiology

Recordings of excitatory post-synaptic currents (EPSCs) were performed using whole-cell voltage-clamp. Neurons were clamped at -70 mV using patch pipettes (3–5 M Ω) containing an internal solution comprised of (in mM): 140 CsCl, 10 EGTA, 5 HEPES, 2 CaCl₂, 2 MgATP, 0.3 NaGTP, 3 QX314Cl (pH 7.3, 280–285 mOsm/L). EPSCs were evoked via small tungsten bipolar stimulating electrodes (FHC, Bowdoin, ME, USA) placed in the BLA (rate = 0.033–0.050 Hz; stimuli, 0.5–100 V, 100 μ s). All evoked EPSCs were recorded in the presence of the GABA_A receptor antagonists SR-95531 (10 μ M) and picrotoxin (100 μ M) to block fast inhibitory synaptic transmission.

Data collection and analysis

All recorded signals were amplified, low pass filtered (5 kHz), digitised and acquired (sampled at 10 kHz) using Multiclamp 700B amplifier (Molecular Devices) and online/offline analysis was performed with Axograph Acquisition software (Molecular Devices). In all experiments, series resistance was monitored and cells were discarded if resistance was >20 M Ω or fluctuated by more than 20%. The number of experiments were not planned before any data was obtained, thus the current study is of an exploratory nature. For this type of experiment we would typically obtain $n = 5-7$ but numbers may vary due to effect size or variability. In addition some control experiments have higher replicates. As follows, the data analysis was preplanned. All eEPSCs were analysed with respect to peak amplitude. Peak amplitude was quantified as the mean peak amplitude of 4-8 eEPSCs, after responses reached a stable plateau. Paired pulse ratio (PPR) was calculated from the peak amplitudes of eEPSCs elicited by paired stimulating pulses (50 ms interpulse interval, second eEPSC/first eEPSC). Effects of exogenously applied drugs are represented as percentage inhibition, which reflects the difference between mean amplitude during drug superfusion and baseline. Reversal of drug effects by antagonists were calculated as the proportion of the baseline amplitude recovered during the washout or antagonist application over the

total eEPSC amplitude lost during drug superfusion. No outliers were removed from analysis.

Statistical analysis was determined before any results were obtained. Statistical analysis was performed using Prism (GraphPad Software, San Diego, CA). Results were analysed as follows. Differences between individual drug effects and baseline were analysed using unpaired Student's *t*-tests. Drug effects within the same cells were analysed using paired Student's *t*-tests. The difference between drug effects with respect to baseline were analysed using one-way repeated measures ANOVAs followed by Bonferroni's tests for multiple comparisons. All statistical tests and results are indicated in figure legends. *p* values < 0.05 were regarded as significant. Data are expressed as mean ± SD or when expressed as percent inhibition are shown as mean with lower-upper 95% confidence interval (CI) of mean.

Drugs

All drugs were diluted to their final concentration in ACSF and applied by superfusion. Concentrations of 6-Imino-3-(4-methoxyphenyl)-1(6*H*)-pyridazinebutanoic acid hydrobromide (SR-95531; 10 μM; Abcam, Cambridge, UK), picrotoxin (100 μM; Sigma, St. Louis, Missouri, USA) methionine-enkephalin (met-enk; 100 nM; Sigma, St. Louis, Missouri, USA), naloxone (10 μM; Tocris, Bristol, UK), thiorphan (10 μM; Abcam, Cambridge, UK), bestatin (10 μM; Abcam, Cambridge, UK), captopril (1 μM; Sigma, St. Louis, Missouri, USA) and (±)-1-[(3*R**,4*R**)-1-(Cyclooctylmethyl)-3-(hydroxymethyl)-4-piperidiny]-3-ethyl-1,3-dihydro-2*H*-benzimidazol-2-one (J113397; 1 μM; Tocris, Bristol, UK) remained the same for all experiments. Nociceptin/Orphanin FQ (N/OFQ; 100 nM, 300 nM, 1 μM, 3 μM; Tocris, Bristol, UK) concentration was varied where indicated.

Results

Enkephalin-degrading peptidases control met-enk actions at the BLA-Im synapse

In the current paper, we indirectly measured peptidase activity in order to determine the level of control they exert over opioid activity at the BLA-Im synapse. By electrically stimulating the BLA, we recorded the resulting eEPSCs from Im neurons using whole-cell patch-clamp electrophysiology (Figure 1B). Then, by applying a cocktail of enkephalin-degrading peptidase inhibitors (PI cocktail) to our slices we were able to examine the extent to which these peptidases collectively regulate enkephalin activity. Our PI cocktail consisted of: thiorphan (10 μ M), captopril (1 μ M) and bestatin (10 μ M) which respectively inhibit NEP (Roques et al., 1980, Rose et al., 2002, Table 1), ACE (Dalkas et al., 2010) and APN (Rich et al., 1984; Figure 1A, Table 1). The concentration of thiorphan was chosen to inhibit both isoforms of NEP (Table 1). Although thiorphan and captopril have been reported to display inhibitory activity at other peptidases they are most selective for our peptidases of interest (Table 1). Thus, thiorphan and captopril sensitive responses could be predominately attributable to NEP and ACE. In these experiments a submaximal concentration of met-enk was chosen so that, if peptidase inhibition increased extracellular met-enk concentrations, we could observe the resulting increase in synaptic inhibition (Figure 1C). At the BLA-Im synapse, a submaximal concentration of met-enk (100nM) modestly, yet consistently, inhibits baseline eEPSC amplitude (baseline: 107.61 \pm 63.64 pA vs. met-enk: 80.39 \pm 52.26 pA, $p < 0.0001$, paired Student's t -test, Figure 1D,E). This inhibition was accompanied by an increase in paired pulse ratio, indicating a presynaptic site of met-enk action (baseline: 1.59 \pm 0.68 vs. met-enk: 1.94 \pm 0.87, $p = 0.0107$, paired Student's t -test, Figure 1F). Application of the PI cocktail significantly enhances the ability of submaximal met-enk to inhibit eEPSC amplitude (met-enk: 15.04%, 95% CI 7.06-23.02, met-enk + PI cocktail: 55.57%, 95% CI 44.41-66.74, met-enk + PI cocktail + naloxone: -2.73%, 95% CI -17.71-12.26 $p < 0.01$, one-way ANOVA, Figure 1G,H), with

an increase in paired pulse ratio also being observed during inhibitor application (baseline: 1.80 ± 1.34 vs. PI cocktail: 3.78 ± 2.23 , $p < 0.05$, paired Student's *t*-test, Figure 1I). The findings are consistent with our previous data (Winters et al., 2017) that show enhanced opioid inhibition of synaptic transmission at the BLA-Im synapse following pharmacological inhibition of the three enkephalin-degrading peptidases.

Paired pulse stimulation of the BLA releases endogenous opioids in the Im, however, the amount of peptide released by this low stimulation is too rapidly degraded to exert any measurable effect (Winters et al., 2017). Thus, we administered the PI cocktail to the BLA-Im synapse alone in order to see whether we could protect endogenous opioids from degradation and observe their activity. When the PI cocktail was applied to slices in the absence of met-enk, it had little effect on baseline synaptic transmission (baseline: 155.44 ± 72.03 pA, $n = 7$ vs. PI cocktail 139.24 ± 80.72 pA, $n = 7$, inhibition = 12.92%, 95% CI -0.20-26.05, paired Student's *t*-test, $p = 0.14$). This suggests that any further increase to the level of met-enk inhibition by the PI cocktail can be interpreted as predominately due to protection of exogenous met-enk from degradation.

NEP is the critical enkephalin-degrading peptidase at the BLA-Im synapse

While all three of the enkephalin-degrading peptidases are expressed in the amygdala (Pollard et al., 1989; Krizanova et al., 2001; Banegas et al., 2005), it is unknown which specific peptidase is crucial for met-enk degradation at the BLA-Im synapse. Thus, we sought to determine the relative contribution of enkephalin-degrading peptidases to the prevention of enkephalinergic signalling through opioid receptors at the BLA-Im synapse by testing each peptidase inhibitor individually. Figure 2 shows that the application of 1 μ M captopril (Figure 2A,B,C) or 10 μ M bestatin (Figure 2D,E,F) provided met-enkephalin with no protection against peptidase degradation. The addition of 10 μ M thiorphan however, significantly increased the extent of met-

enkephalin inhibition (met-enk: 28.65%, 95% CI 13.87-43.44, met-enk + thiorphan: 55.80%, 95% CI 46.15-65.44, met-enk + thiorphan + naloxone: 8.13%, 95% CI -0.65-16.91, $p < 0.05$, one-way ANOVA, Figure 2G,H,I). Moreover, this enhanced inhibition was comparable to that observed with the combined application of all three peptidases (PI cocktail: 55.57%, 95% CI 46.15-65.44, $n=5$ vs. thiorphan alone: 55.80%, 95% CI 44.41-66.74, $n=6$, $p = 0.97$, unpaired Student's t -test), suggesting met-enk was protected from peptidase breakdown to a similar degree. Together, these results indicate that the peptidase targeted by thiorphan (NEP) is both necessary and sufficient for substantial met-enkephalin degradation at the BLA-Im synapse.

NEP regulation of synaptic transmission at the BLA-Im traverses peptide systems

Although NEP has been termed an enkephalinase and changes in NEP activity can increase and/or decrease enkephalin levels to the extent that endogenous opioid-related behaviours such pain responses, behavioural despair, and conditioned reinforcement are altered (Schwartz et al., 1985), NEP is not exclusively selective for enkephalin. In fact, NEP has a wide anatomical distribution (Bayes-Genis et al., 2016) and a broad substrate selectivity and can cleave various peptide targets including, but not limited to tachykinins (Matsas et al., 1983), neurotensin (Kitabgi et al., 1992), natriuretic peptides (Schwartz et al., 1990) and cholecystikinin (Matsas et al., 1984). One such candidate substrate is nociceptin/orphanin FQ (N/OFQ) – an opioid-like neuropeptide with some sequence similarity to the endogenous opioid, dynorphin. Like endogenous opioids, N/OFQ has a glycine-phenylalanine bond, is degraded by NEP in membrane fragments (Sakurada et al., 2002) and is expressed in the amygdala (Neal et al., 1999). We took advantage of these parallels in order to investigate whether NEP regulation of peptide activity at the BLA-Im synapse was restricted to opioids or whether it would extend to regulation of other neuropeptides. First, we determined the effect of N/OFQ on glutamate release at the BLA-Im. We found that in untreated tissue,

N/OFQ produced a concentration-dependent inhibition of eEPSCs (Figure 3A). At the maximal concentration, N/OFQ inhibition was accompanied by an increase in PPR, however this was not observed at lower concentrations (baseline: 1.02 ± 0.13 , N/OFQ: 1.33 ± 0.21 , $p < 0.05$, paired Student's *t*-test, Figure 3B). The N/OFQ inhibition of eEPSC amplitude was reversed by the N/OFQ receptor antagonist J113397 (Figure 3D). These data indicate that, in a manner analogous to endogenous opioids, the BLA-Im synapse is regulated by N/OFQ.

By taking advantage of our established submaximal N/OFQ concentration (100 nM) and then applying thiorphan (10 μ M) to slices, we tested whether NEP could also regulate N/OFQ signalling at the BLA-Im synapse. In all cells, the submaximal N/OFQ inhibition was enhanced following thiorphan application (N/OFQ: 17.04%, 95% CI 1.21-32.88, N/OFQ + thiorphan: 28.98%, 95% CI 13.54-44.43, N/OFQ + thiorphan + J113397: 2.97%, 95% CI -2.23-8.17, $p < 0.05$, one-way ANOVA, Figure 3C,D). However, unlike met-enk, thiorphan application did not change PPR (Figure 3E). Together these data indicate NEP also targets N/OFQ for degradation in the intercalated cells of the amygdala.

Discussion

The present results demonstrate that peptidase degradation of met-enk limits the extent of opioid inhibition of synaptic glutamate release to the intercalated cells of the amygdala. We tested inhibitors of the three main classes of enkephalin degrading peptidases and found that inhibition of NEP alone could enhance enkephalin responses to the same extent as inhibitors of all three peptidases combined. The potentiation of opioid inhibition in intercalated cells by thiorphan alone indicates that inhibition of NEP prevents cleavage of the Gly-Phe bond, which is sufficient to protect enkephalin from degradation. The failure of bestatin and captopril to alter the level of met-enk inhibition, suggests that neither APN nor ACE activity can sufficiently change enkephalin concentrations at synaptic opioid receptors enough to alter glutamate release.

The current results, indicating the dominance of NEP in metabolism of enkephalins in the intercalated cells, differs from the multiple peptidases responsible for enkephalin metabolism in *in vitro* membrane fragments from the striatum (Guyon et al., 1979; Malfroy et al., 1978; Hiranuma and Oka, 1986; Hiranuma et al., 1997, 1998) but also differs from what has been seen in other brain regions using cellular readouts of opioid receptor activity. For example, in the locus coeruleus (Williams et al., 1987) and spinal cord (Song and Marvizon, 2003), enkephalin degradation relies on multiple or alternative peptidases. It may be that the differential peptidase activity in membrane fragments arises from the contribution of intracellular peptidases which would not participate in our experiments. However, this cannot explain the difference between the current results and results from experiments using cellular readouts of opioid receptor function (Williams et al., 1987; Song and Marvizon, 2003). We suggest there are three possible explanations for this difference. Firstly, that there is heterogenous expression of enkephalin-degrading peptidases in discrete neural circuits. Although there is widespread distribution of all three peptidases in the brain at the macroscopic

level, the dominance of NEP in the intercalated cells may result from higher microscopic expression of NEP in amygdala nuclei compared to other brain peptidases. Indeed, immunohistochemical and radiochemical mapping of NEP in the CNS have shown higher patterns of NEP expression and activity within amygdala nuclei (Pollard et al., 1989; Waksman et al., 1986) compared to only moderate and/or negligible levels of ACE (Strittmatter et al., 1984; Chai and Paxinos, 1987) and APN (Noble et al., 2001; Banegas et al., 2005). By contrast, only low to moderate levels of NEP and high levels of ACE and APN have been observed in brain regions such as the locus coeruleus and spinal cord where enkephalin degradation relies on multiple peptidases (Pollard et al., 1989; Facchinetti et al., 2003; Noble et al., 2001). A second possible explanation is that only synaptic enkephalin concentrations, as measured here, are determined by NEP in the intercalated cells, whereas the other enkephalin-degrading enzymes may contribute to enkephalin breakdown at other cellular locations such as the cell body or dendrites, or even intracellularly (Williams et al., 1987, Song and Marvizon, 2003). If this is the case, subcellular localisation, in addition to regional distribution, should be considered when elucidating the physiological control of peptides by peptidases. The third possible explanation for the dominance of NEP in the intercalated cells is more speculative but warrants consideration. As we showed in this study, NEP also controls the synaptic concentrations of N/OFQ in the intercalated cells. Likewise, APN and ACE have a broad substrate specificity and degrade peptides with susceptible peptide bonds such as substance P (Hooper and Turner, 1985), neurokinins (Marvizon et al., 2003), angiotensin and bradykinin (Dorer et al., 1974) and cholecystokinin (Matsas et al., 1984). Given this, if any of the other peptides targeted by APN and ACE are present at significant synaptic concentrations in the intercalated cells, they may compete with enkephalin for degradation and thus limit APN and ACE effects. Regardless of the mechanism, this data suggests that the mechanisms by which neuropeptides are metabolised, either in membrane fragments or in other regions of the CNS, cannot be generalised. Thus, in order to appropriately determine

the influence of peptidases over peptide actions in the CNS, tissue from specific regions of interest containing: 1) native levels of peptidase activity, 2) intact cellular microarchitecture, and 3) other peptides targeted by the peptidase of interest must be used.

In this study we examined peptidase control of enkephalin under control conditions. However, many factors can alter peptidase expression and activity, including chronic morphine treatment (Malfroy et al., 1978), stress (Hernández et al., 2009), stroke (Kerridge et al., 2015) and increasing age/Alzheimers disease (Reilly, 2001). Given the location specificity we have defined in this study it would be interesting to test whether disease pathology changes peptidase activity, and thus peptide level, and whether these changes occur globally or at specific locations. Defining the specific peptidase and how it may change in a disease state would allow rationale choices of drugs targeting the specific peptidase of interest. For example, increases in NEP activity within the amygdala could be usefully targeted using currently available drugs to regulate endogenous opioid actions in drug addiction, pain or fear disorders.

Author contributions

Participated in research design: Gregoriou and Bagley

Conducted experiments: Gregoriou, Winters and Patel

Performed data analysis: Gregoriou and Bagley

Wrote or contributed to writing of manuscript: Gregoriou and Bagley

References

- Banegas I, Prieto I, Alba F, Vives F, Araque A, Segarra AB, Durán R, de Gasparo M, Ramírez M (2005) Angiotensinase activity is asymmetrically distributed in the amygdala, hippocampus and prefrontal cortex of the rat. *Behav Brain Res* **156(2)**: 321-6
- Barnes K, Matsas R, Hooper NM, Turner AJ, Kenny AJ (1988). Endopeptidase-24.11 is striosomally ordered in pig brain and, in contrast to aminopeptidase n and peptidyl dipeptidase a ('angiotensin converting enzyme'), is a marker for a set of striatal efferent fibres. *Neuroscience* **27(3)**: 799-817
- Bayes-Genis A, Barallat J, Richards AM (2016) A Test in Context: Neprilysin: Function, Inhibition, and Biomarker. *J Am Coll Cardiol* **68(6)**: 639-653
- Bodnar RJ (2018) Endogenous Opiates and Behavior: 2016. *Peptides* **101**: 167-212
- Chai SY, Mendelsohn FAO, Paxinos G (1987) Angiotensin converting enzyme in rat brain visualized by quantitative in vitro autoradiography *Neuroscience* **20(2)**: 615-627
- Chou J, Tang J, Del Rio J, Yang HY, Costa E (1984) Action of peptidase inhibitors on methionine5-enkephalin-arginine6-phenylalanine7 (YGGFMRF) and methionine5-enkephalin (YGGFM) metabolism and on electroacupuncture antinociception. *J Pharmacol Exp Ther* **230(2)**: 349-52
- Dalkas GA, Marchand D, Galleyrand JC, Martinez J, Spyroulias GA, Cordopatis P, Cavellier F. (2010). Study of a lipophilic captopril analogue binding to angiotensin I converting enzyme. *J Pept Sci* **16(2)**: 91-97

Dorer FE, Kahn JR, Lentz KE, Levine M, Skeggs LT (1974) Hydrolysis of bradykinin by angiotensin-converting enzyme. *Circ Res* **34(6)**: 824-7

Erdös EG, Johnson AR, Boyden NT (1978) Hydrolysis of enkephalin by cultured human endothelial cells and by purified peptidyl dipeptidase. *Biochem Pharmacol* **27(5)**: 843-8

Facchinetti P, Rose C, Schwartz JC, Ouimet T (2003) Ontogeny, regional and cellular distribution of the novel metalloprotease neprilysin 2 in the rat: a comparison with neprilysin and endothelin-converting enzyme-1. *Neuroscience* **118(3)**: 627-639

Foulon T, Cadel S, Chesneau V, Draoui M, Prat A, Cohen P. (1996). Two Novel Metallopeptidases with a Specificity for Basic Residues Functional Properties, Structure, and Cellular Distribution. *Ann N Y Acad Sci* **22(780)**:106-20

Giros B, Gros C, Solhonne B, Schwartz J. (1985). Characterization of Aminopeptidases Responsible for Inactivating Endogenous (Met⁵)Enkephalin in Brain Slices Using Peptidase Inhibitors and Anti-Aminopeptidase M Antibodies. *Mol Pharmacol* **29**: 281-287

Gros C, Giros B, Schwartz JC (1985) Purification of membrane-bound aminopeptidase from rat brain: identification of aminopeptidase M. *Neuropeptides*, **5(4-6)**: 485-488

Guyon A, Roques BP, Guyon F, Foucault A, Perdrisot R, Swerts JP, Schwartz JC (1979) Enkephalin degradation in mouse brain studied by a new H.P.L.C. method: further evidence for the involvement of carboxydipeptidase. *Life Sci* **25(18)**: 1605-11

Hernández J, Segarra AB, Ramírez M, Banegas I, de Gasparo M, Alba F, Vives F, Durán R, Prieto I. (2009) Stress influences brain enkephalinase, oxytocinase and angiotensinase activities: a new hypothesis. *Neuropsychobiology*, **59(3)**:184-9.

Hersh LB (1985) Characterization of membrane-bound aminopeptidases from rat brain: identification of the enkephalin-degrading aminopeptidase. *J Neurochem* **44(5)**: 1427-35

Hiranuma T, Oka T (1986) Effects of peptidase inhibitors on the [Met5]-enkephalin hydrolysis in ileal and striatal preparations of guinea-pig: almost complete protection of degradation by the combination of amastatin, captopril and thiorphan. *Jpn J Pharmacol* **41(4)**: 437-46

Hiranuma T, Iwao K, Kitamura K, Matsumiya T, Oka T (1997) Almost complete protection from [Met5]-enkephalin-Arg6-Gly7-Leu8 (Met-enk-RGL) hydrolysis in membrane preparations by the combination of amastatin, captopril and phosphoramidon. *J Pharmacol Exp Ther* **281(2)**: 769-74

Hiranuma T, Kitamura K, Taniguchi T, Kobayashi T, Tamaki R, Kanai M, Akahori K, Iwao K, Oka T (1998) Effects of three peptidase inhibitors, amastatin, captopril and phosphoramidon, on the hydrolysis of [Met5]-enkephalin-Arg6-Phe7 and other opioid peptides. *Naunyn Schmiedebergs Arch Pharmacol* **357(3)**: 276-82

Hooper NM, Kenny AJ, Turner AJ (1985) The metabolism of neuropeptides. Neurokinin A (substance K) is a substrate for endopeptidase-24.11 but not for peptidyl dipeptidase A (angiotensin-converting enzyme). *J Biochem* **231(2)**: 357–361

Inguibert N, Coric P, Poras H, Meudal H, Teffot F, Fournié-Zaluski M, Roques BP (2002) Toward an optimal joint recognition of the S1' subsites of endothelin converting enzyme-1 (ECE-1), angiotensin converting enzyme (ACE), and neutral endopeptidase (NEP). *J Med Chem* **45(7)**: 1477-1486

Janak PH, Tye KM (2015) From circuits to behaviour in the amygdala. *Nature* **517(7534)**: 284-92

Kerridge C, Kozlova DI, Nalivaeva NN, Turner AJ (2015) Hypoxia Affects Nephilysin Expression Through Caspase Activation and an APP Intracellular Domain-dependent Mechanism. *Front Neurosci.* **13;9**:426.

Kitabgi P, Dubuc I, Nouel D, Costentin J, Cuber JC, Fulcrand H, Doulut S, Rodriguez M, Martinez J (1992) Effects of thiorphan, bestatin and a novel metallopeptidase inhibitor JMV 390-1 on the recovery of neurotensin and neuromedin N released from mouse hypothalamus. *Neurosci Lett* **142(2)**: 200-4

Krizanova O, Kiss A, Zacikova L, Jezova D (2001) Nitric oxide synthase mRNA levels correlate with gene expression of angiotensin II type-1 but not type-2 receptors, renin or angiotensin converting enzyme in selected brain areas. *Physiol Res* **50**: 473-480

Leyhausen G, Schuster DK, Vaith P, Zahn RK, Umezawa H, Falke D, Müller WEG. (1983). Identification and properties of the cell membrane bound leucine aminopeptidase interacting with the potential immunostimulant and chemotherapeutic agent bestatin. *Biochem Pharmacol* **32(6)**: 1051-1057

Lutz PE1, Kieffer BL (2013) Opioid receptors: distinct roles in mood disorders.

Trends Neurosci **36(3)**: 195-206

Malfroy B, Swerts JP, Guyon A, Roques BP, Schwartz JC (1978) High-affinity enkephalin-degrading peptidase in brain is increased after morphine. *Nature*

276(5687): 523-6

Marvizon JC, Wang X, Lao LJ, Song B (2003) Effect of peptidases on the ability of exogenous and endogenous neurokinins to produce neurokinin 1 receptor

internalization in the rat spinal cord. *Br J Pharmacol* **140(8)**: 1389-98

Matsas R, Fulcher IS, Kenny AJ, Turner AJ (1983) Substance P and [Leu]enkephalin are hydrolyzed by an enzyme in pig caudate synaptic membranes that is identical

with the endopeptidase of kidney microvilli. *PNAS* **80(10)**: 3111-5

Matsas R, Turner AJ, Kenny AJ (1984) Endopeptidase-24.11 and aminopeptidase activity in brain synaptic membranes are jointly responsible for the hydrolysis of

cholecystokinin octapeptide (CCK-8). *FEBS Lett* **175(1)**: 124-8

Melzig MF, Bormann H. (1988). Betulinic acid inhibits aminopeptidase N

activity. *Planta Med* **64(7)**: 655-657

Miyamoto A, Murata S, Nishio A. (2002). Role of ACE and NEP in bradykinin-induced relaxation and contraction response of isolated porcine basilar artery. *Arch*

Pharmacol **365**: 365–370

- Neal CR, Mansour A, Reinscheid R, Nothacker HP, Civelli O, Watson SJ (1999) Localization of orphanin FQ (nociceptin) peptide and messenger RNA in the central nervous system of the rat. *J Comp Neurol* **406(4)**: 503-47
- Noble F, Banisadr G, Jardinaud F, Popovici T, Lai-Kuen R, Chen H, Bischoff L, Parsadaniantz SM, Fournie-Zaluski MC, Roques BP (2001) First discrete autoradiographic distribution of aminopeptidase N in various structures of rat brain and spinal cord using the selective iodinated inhibitor [¹²⁵I]RB 129. *Neuroscience* **105(2)**: 479-88
- Örning L, Krivi G, Bild G, Gierse J, Aykent S, Fitzpatrick FA. (1991). Inhibition of leukotriene A₄ hydrolase/aminopeptidase by captopril. *J Biol Chem* **266(25)**: 16507-16511
- Örning L, Krivi G, Fitzpatrick FA. (1991). Leukotriene A₄ hydrolase. Inhibition by bestatin and intrinsic aminopeptidase activity establish its functional resemblance to metallohydrolase enzymes. *J Biol Chem* **266(3)**: 1375-1378
- Palmieri FR, Bausback HH, Ward PE. (1989). Metabolism of vasoactive peptides by vascular endothelium and smooth muscle aminopeptidase M. *Biochem Pharmacol* **38(1)**: 173-180
- Pollard H, Bouthenet ML, Moreau J, Souil E, Verroust P, Ronco P, Schwartz JC (1989) Detailed immunautoradiographic mapping of enkephalinase (EC 3.4.24.11) in rat central nervous system: comparison with enkephalins and substance P. *Neuroscience* **30(2)**: 339-76

Reilly CE (2001). Neprilysin content is reduced in Alzheimer brain areas. *J. Neurol.* **248**, 159–160.

Rich DH, Moon BJ, Harbeson S. (1984). Inhibition of aminopeptidases by Amastatin and Bestatin derivatives. Effect of inhibitor structure on slow-binding processes. *J Med Chem* **27(4)**: 418-422

Roques BP, Fournié-Zaluski MC, Sorooca E, Lecomte JM, Malfroy B, Llorens C, Schwartz JC (1980) The enkephalinase inhibitor thiorphan shows antinociceptive activity in mice. *Nature* **288(5788)**: 286-8

Rose C, Voisin S, Gros C, Schwartz JC, Ouimet T (2002) Cell-specific activity of neprilysin 2 isoforms and enzymic specificity compared with neprilysin. *Biochem J* **363**:697-705.

Sakurada C, Sakurada S, Orito T, Tan-No K, Sakurada T (2002) Degradation of nociceptin (orphanin FQ) by mouse spinal cord synaptic membranes is triggered by endopeptidase-24.11: an in vitro and in vivo study. *Biochem Pharmacol* **8**: 1293-1303

Schwartz J, Costentin J, Lecomte J (1985) Pharmacology of enkephalinase inhibitors. *TIPS* **6**: 472-476

Schwartz JC, Gros C, Lecomte JM, Bralet J (1990) Enkephalinase (EC 3.4.24.11) inhibitors: protection of endogenous ANF against inactivation and potential therapeutic applications. *Life Sci* **47(15)**: 1279-97

Shim JS, Kim JH, Cho HY, Yum YN, Kim SH, Park H, Shim BS, Choi SH, Kwon HJ. (2003). Irreversible Inhibition of CD13/Aminopeptidase N by the Antiangiogenic Agent Curcumin. *Chem & Biol* **10(8)**: 695-704

Song B and Marvizón JCG (2003) Peptidases prevent μ -Opioid receptor internalization in dorsal horn neurons by endogenously released opioids. *J Neurosci* **23(5)**: 1847-1858

Strittmatter SM, Lo MM, Javitch JA, Snyder SH (1984) Autoradiographic visualization of angiotensin-converting enzyme in rat brain with [3 H]captopril: localization to a striatonigral pathway. *PNAS* **81(5)**: 1599-603

Sullivan S, Akil H, Barchas JD (1978) In vitro degradation of enkephalin: evidence for cleavage at the Gly-Phe bond. *Commun Psychopharmacol* **2(6)**: 525-31

Umezawa H, Ayoagi T, Suda H, Hamada M, Takeuchi T. (1975). Bestatin, an inhibitor of aminopeptidase B, produced by actinomycetes. *J Antibiot* **29(1)**: 97-99

Tieku S, Hooper NM. (1992). Inhibition of aminopeptidases N, A and W. A re-evaluation of the actions of bestatin and inhibitors of angiotensin converting enzyme. *Biochem Pharmacol* **44(9)**: 1725-1730

Waksman G, Hamel E, Delay-Goyet P, Roques BP (1986) Neuronal localization of the neprilysin 'enkephalinase' in rat brain revealed by lesions and autoradiography. *EMBO* **5(12)**: 3163-6

Whyteside AR, Turner AJ. (2008). Human neprilysin-2 (NEP2) and NEP display distinct subcellular localisations and substrate preferences. *FEBS*

Lett **582(16)**: 2382-2386

Williams JT, Christie MJ, North RA, Roques BP (1987) Potentiation of enkephalin action by peptidase inhibitors in rat locus ceruleus in vitro. *J Pharmacol Exp Ther*

243(1): 397-401

Winters BL, Gregoriou GC, Kisiwaa SA, Wells OA, Medagoda DI, Hermes SM, Burford NT, Alt A, Aicher SA, Bagley EE (2017) Endogenous opioids regulate moment-to-moment neuronal communication and excitability. *Nat Commun* **8**: 14611

Footnote

This work was supported by the National Health and Medical Research Council (NHMRC) [Grant APP1047372].

Figure Legends

Figure 1. The inhibition of glutamate transmission produced by met-enk at the BLA-Im synapse is enhanced by inhibiting enkephalin-degrading peptidases

(a) Met-enk is catabolised by various peptidases. Diagram shows low affinity cleavage site (*), high affinity cleavage site (**), peptidases in blue (APN: aminopeptidase N; NEP: neprilysin; ACE: angiotensin-converting enzyme) and their corresponding inhibitors in red. (b) Schematic of BLA-Im stimulation and recording sites. Bipolar stimulating electrodes were placed in the BLA and the response of Im neurons to this stimulation was recorded. (c) Graphic showing experimental paradigm. (d) Representative traces showing inhibition of baseline eEPSC amplitude by submaximal met-enk (100 nM). (e) Graph showing percentage inhibition of eEPSC amplitude (from baseline) by submaximal met-enk (100nM) and reversal by naloxone (10 μ M), *** p < 0.001, met-enk vs. baseline, unpaired t -test. (f) Before and after scatter plot of PPR at baseline and submaximal met-enk (100nM), * p = 0.011, baseline vs. met-enk, paired t -test (g) Representative traces showing that inhibition of baseline eEPSC amplitude by submaximal met-enk (100nM) is potentiated by a cocktail of peptidase inhibitors (PI cocktail: thiorphan 10 μ M, bestatin 10 μ M and captopril 1 μ M). (h) Graph showing percentage inhibition of eEPSC amplitude (from baseline) by submaximal met-enk (100nM), PI cocktail (thiorphan 10 μ M, bestatin 10 μ M and captopril 1 μ M) and reversal by naloxone (10 μ M), ** p = 0.0031, met-enk vs. PI cocktail, one-way repeated measures ANOVA followed by Bonferroni's multiple comparisons test, ** p = 0.0070, PI cocktail vs. naloxone, one-way repeated measures ANOVA followed by Bonferroni's multiple comparisons test. (i) Before and after scatter plot of PPR at baseline and during PI cocktail (thiorphan 10 μ M, bestatin 10 μ M and captopril 1 μ M), * p = 0.0457, baseline vs. PI cocktail, paired t -test. Each point on graphs represents a single neuron. Bars on graphs represent the mean.

Figure 2. Effect of individual peptidase inhibitors on met-enk-induced inhibition of glutamate neurotransmission

(a) Representative traces showing baseline amplitude of eEPSC at BLA-Im synapse and inhibition of baseline amplitude following application of submaximal met-enk (100nM) and then captopril (1 μ M). (b) Graph showing percentage inhibition of eEPSC amplitude (from baseline) by submaximal met-enk (100nM), captopril (1 μ M) and reversal by naloxone (10 μ M), * p = 0.0217, met-enk vs. naloxone, one-way repeated measures ANOVA followed by Bonferroni's multiple comparisons test, * p = 0.0154, captopril vs. naloxone, one-way repeated measures ANOVA followed by Bonferroni's multiple comparisons test. (c) Before and after scatter plot of PPR in baseline and captopril. Captopril did not change the PPR, p = 0.1144, paired t -test. (d) Representative traces showing baseline amplitude of eEPSC at BLA-Im synapse and inhibition of baseline amplitude following application of submaximal met-enk (100nM) and then bestatin (10 μ M). (e) Graph showing percentage inhibition of eEPSC amplitude (from baseline) by submaximal met-enk (100nM), bestatin (10 μ M) and reversal by naloxone (10 μ M). ** p = 0.0023, met-enk vs. naloxone, one-way repeated measures ANOVA followed by Bonferroni's multiple comparisons test, *** p = 0.0006, bestatin vs. naloxone, one-way repeated measures ANOVA followed by Bonferroni's multiple comparisons test. (f) Before and after scatter plot of PPR in baseline and bestatin. Bestatin did not change the PPR, p = 0.0835, paired t -test. (g) Representative traces showing baseline amplitude of eEPSC at BLA-Im synapse and inhibition of baseline amplitude following application of submaximal met-enk (100nM) and then thiorphan (10 μ M). (h) Graph showing percentage inhibition of eEPSC amplitude (from baseline) by submaximal met-enk (100nM), thiorphan (10 μ M) and reversal by naloxone (10 μ M). * p = 0.118, met-enk vs. thiorphan, one-way repeated measures ANOVA followed by Bonferroni's multiple comparisons test, *** p = 0.0003, thiorphan vs. naloxone, one-way repeated measures ANOVA followed by Bonferroni's multiple comparisons test. (i) Before and after scatter plot of PPR in baseline and thiorphan.

Thiorphan did not change the PPR, $p = 0.1201$, paired t -test. Each point on graphs represents a single neuron. Bars on graphs represent mean.

Figure 3. Neprilysin blockade enhances actions of nociceptin at BLA-Im synapse

(a) Concentration-response relationship for percent inhibition of eEPSC amplitudes by nociceptin/orphanin FQ (N/OFQ) at the BLA-Im synapse. Each point shows the mean \pm 95% CI of five neurons. A logistic function was fitted to the concentration-response curve. (b) Before and after scatter plot of PPR in baseline and maximal N/OFQ (3 μ M), $*p = 0.0345$, baseline vs. N/OFQ (3 μ M), paired t -test (c) Representative traces showing baseline amplitude of eEPSC at BLA-Im synapse and inhibition of baseline amplitude following application of submaximal N/OFQ (100nM) and then thiorphan (10 μ M). (d) Graph showing percentage inhibition of eEPSC amplitude (from baseline) by submaximal N/OFQ 100nM), thiorphan (10 μ M) and reversal by the selective NOP receptor antagonist J113397 (1 μ M). $***p = 0.0010$, N/OFQ vs. thiorphan, one-way repeated measures ANOVA followed by Bonferroni's multiple comparisons test, $*p = 0.0376$, thiorphan vs. J113397, one-way repeated measures ANOVA followed by Bonferroni's multiple comparisons test. (e) Before and after scatter plot of PPR in baseline and thiorphan (10 μ M). Thiorphan did not change the PPR, $p = 0.2177$, paired t -test. Each point on graphs represents a single neuron. Bars on graphs represent mean.

Table 1. Selectivity of peptidase inhibitors

Inhibitor	Peptidase source	NEP	NEP1	NEP2	APN	ACE	Reference
Thiorphan	Striatal membranes	4.7nM				150nm	Roques et al., 1980
	Not stated	4nM				>100nM	Inguibert et al, 2002
	Expressed human		6.9nM	22µM			Whyteside and Turner, 2008
	Expressed rat	4nM		120-250nM			Rose et al., 2002
	Porcine basilar artery	1.4nM				295nM	Miyamoto et al., 2002
Bestatin	Brain membranes				0.5-4µM		Gros 1985
	Porcine kidney				4.1µM		Rich et al., 1984
Captopril	Striatal membranes	10µM				7nm	Roques et al, 1980
	Expressed human					6.3nM	Dalkas et al., 2010
	Porcine basilar artery					38nM	Miyamoto et al., 2002
	Not stated	>1000nM				2nM	Inguibert et al, 2002

Figures

Figure 1

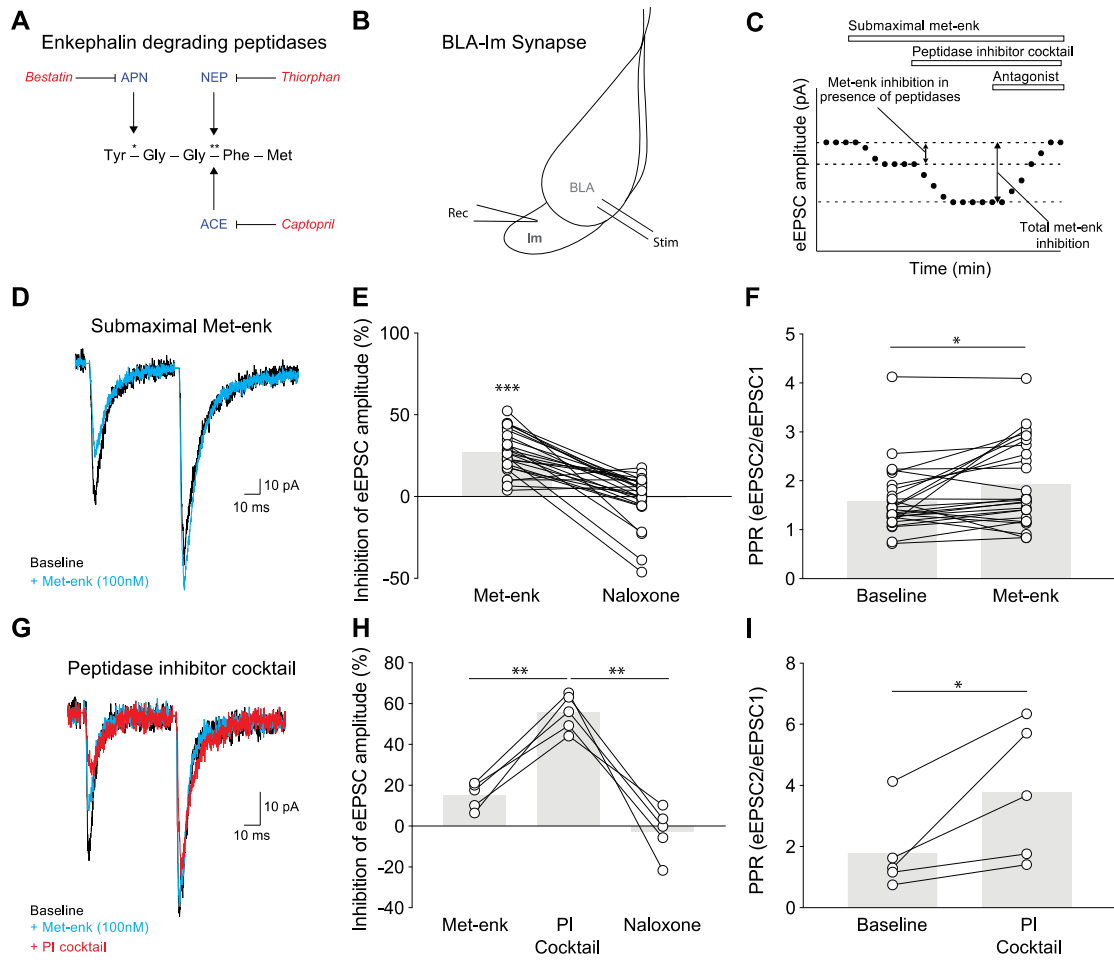


Figure 2

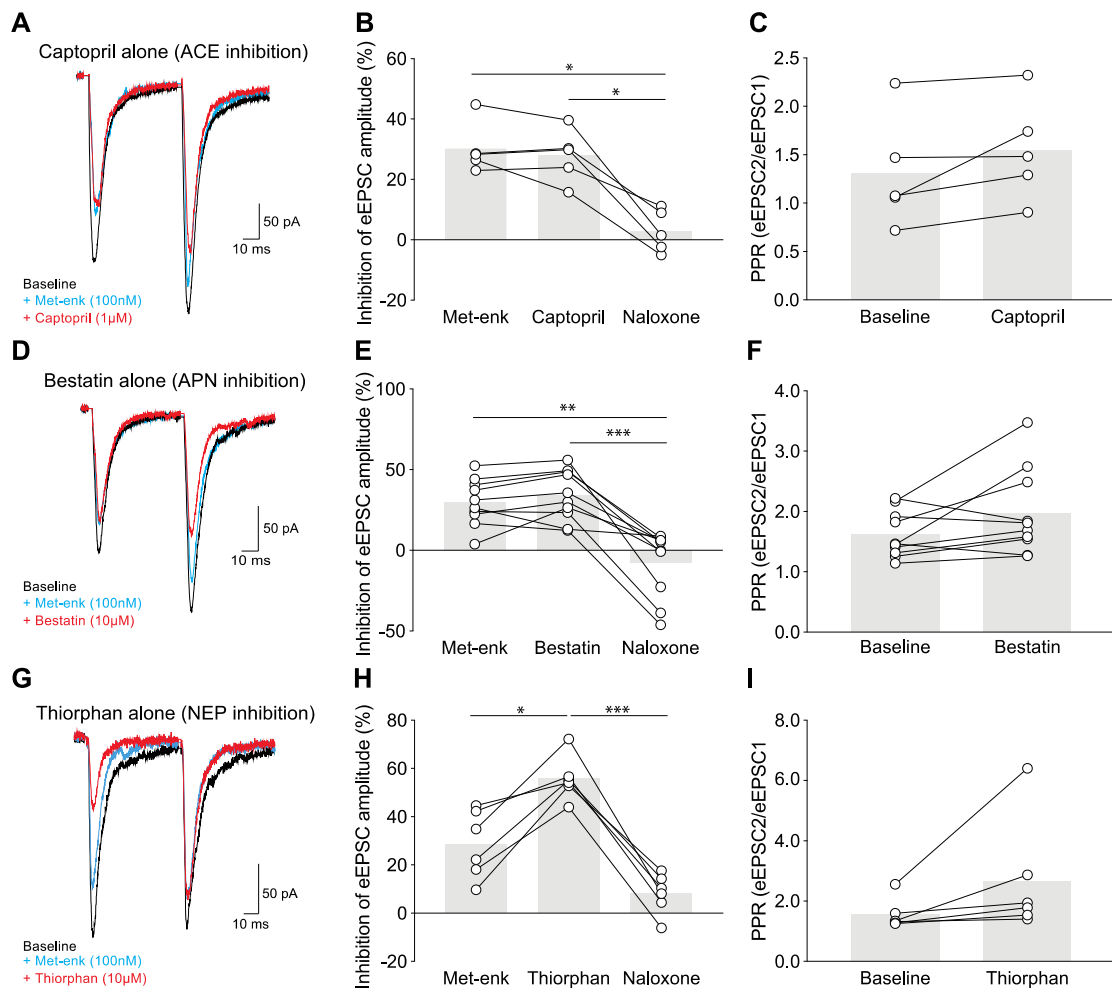


Figure 3

